GMR
The Original

GREEN FABRICATION OF CURDLAN NANOPARTICLES FOR KAEMPFEROL DELIVERY: A SUSTAINABLE APPROACH TO BREAST AND CERVICAL CANCER THERAPY

SARANYA M.V[1], SUDHA T*

[1]Research Scholar, Department of Chemistry and Analysis, Vels Institute of Science, Technology and Advance Studies (VISTAS), Pallavaram, Tamil Nadu, India.
*Department of Chemistry and Analysis, Vels Institute of Science, Technology and Advance Studies (VISTAS), Pallavaram, Tamil Nadu, India
M.V Saranya https://orcid.org/0009-0001-1017-3728
T. Sudha https://orcid.org/0000-0001-8821-3999
*Corresponding Author:
Dr.T.Sudha, M.Pharm, Ph.D,
Associate professor, Department of Pharmaceutical Chemistry and Analysis, School of Pharmaceutical sciences, Vels Institute of Science, Technology and Advanced Studies (VISTAS), Chennai, Tamilnadu, India.

ABSTRACT

Objective
The goal of the current study was to use factorial design to prepare and optimize curdlan nanoparticles loaded with curdlan for targeted drug delivery. A systematic investigation was conducted into the effects of major preparation variables, polymer amount, sodium tripolyphosphate quantity, and stirring speed on drug content, encapsulation efficiency, and cumulative drug release.
Methods
Using TPP as a crosslinker and curdlan as a biodegradable polymer, kaempferol loaded curdlan nanoparticles were created via an altered ionic gelation process. The formulation parameters were optimized using a factorial design. A number of nanoparticle characteristics, such as cumulative drug release, encapsulation effectiveness, and particle size, were described. The prepared nanoparticles morphology was examined using a scanning electron microscope. Additionally, the MTT assay was used to evaluate cytotoxicity on the HeLa and MCF-7 cancer cell line human for cervical and breast cancer.
Results
Particle size of 157.4 nm, drug content of 97.19 %, encapsulation efficiency of 90.45%, cumulative drug release of 95.94 ±0.28 %, Poly Dispersity Index of 0.248, and zeta potential of -25.9 mV are all characteristics of the optimal formulation. The nanoparticles spherical shape was revealed by the SEM results. Studies on in vitro cytotoxicity revealed that the curdlan nanoparticles loaded with kaempferol demonstrated strong anticancer properties, with IC_{50} values of 73.02 µg/ml for MCF-7 and 84.83 µg/ml for HeLa cell lines. Formulations utilizing pharmaceutical-grade kaempferol (≥98% purity) and curdlan (≥90% purity) were considered for inclusion. Only nanoparticles with a particle size below 200 nm, PDI of ≤0.3, drug content of at least 80%, and encapsulation efficiency of ≥70% were selected. Cytotoxicity evaluations were conducted using actively proliferating, contamination-free MCF-7 and HeLa cell lines exhibiting a minimum of 95% viability.
Conclusion
Therefore, it is possible that the newly discovered nanoparticles for the treatment of breast and cervical cancer represents a ground-breaking approach. These findings significantly support the possibility of using these nanoparticles as a therapeutic treatment for breast and cervical cancer patients undergoing or following resection of malignant lesions.

KEYWORDS: Kaempferol, Curdlan nanoparticles, BBD, MTT assay.

INTRODUCTION

Since cancer continues to be a major cause of morbidity and death globally, researchers are looking for safer and more effective treatment approaches. Natural bioactive compounds [1]. such as flavonoids, have attracted significant interest due to their potential as anticancer agents with fewer side effects. These include kaempferol, a dietary flavonoid [2] present in a variety of fruits and vegetables that has shown impressive anticancer qualities, such as the capacity to trigger apoptosis, prevent cell division, and alter important signaling pathways in a number of cancer cell lines, such as MCF-7 and HeLa cells [3-4].

Although kaempferol has medicinal potential, its poor water solubility and bioavailability prevent it from being used in clinical settings. Drug delivery systems based on nanoparticles have been investigated to improve the drug solubility, stability, and targeted distribution in order to get around these restrictions. The gel-forming ability and immunomodulatory qualities of curdlan, a biocompatible and biodegradable β-glucan polysaccharide, have made it a viable carrier material [5-6].

Formulation optimization plays a critical role in developing effective nanocarrier systems. The (BBD) Box–Behnken design, a RSM response surface methodology, offers a statistically efficient and economical approach to optimizing multiple formulation variables simultaneously. It has been widely used to enhance the performance of nanoparticle formulations by identifying optimal conditions for parameters such as zeta potential, particle size, loading drug, and encapsulation efficiency [7].

The current study involved the formulation and optimization of curdlan nanoparticles loaded with kaempferol utilizing BBD, followed by a thorough physicochemical evaluation. By using in vitro cytotoxicity tests on the breast cancer cell line MCF-7 and the cervical cancer cell line HeLa, the optimized nanoparticles anticancer activity was assessed, offering insights into their potential as a novel cancer therapeutic delivery method [8-10].

MATERIALS AND METHODS

Kaempferol-loaded curdlan nanoparticles were made using techniques based on the ionic gelation of curdlan TPP anions, with some modifications. An acetic acid aqueous solution of (0.1 %, v/v) was used to dissolve curdlan (0.2 %, w/v). A 20 % w/v aqueous NaOH solution was used to bring the curdlan solutions pH down to 4.8. Ultrapure water was used to dissolve TPP (0.2%, w/v). To make kaempferol-loaded nanoparticles, kaempferol solution was added while being magnetically stirred to 10 milliliters of the curdlan solution that had been heated to 60 degrees Celsius for ten minutes. Subsequently, 3.3 ml of 4°C TPP solution was dropwise added to a room-temperature curdlan/kaempferol solution while being stirred magnetically for 30 minutes. Opalescent suspension developed on its own. After centrifuging the nanoparticle suspension for 30 minutes at 12,000 rpm, the unencapsulated compounds were removed by washing it with water. To prevent particle aggregation, the suspension of nanoparticles was sonicated for ten minutes following centrifugation. Curdlan and TPP solution without kaempferol solution were used in the above-described procedure to create the empty curdlan/TPP nanoparticles.

IN-VITRO EVALUATION

Zeta potential and Particle size (Malvern zeta sizer)

The Curdlan samples loaded with kaempferol were sonicated, mixed with distilled water, and then left for 30 minutes. The analysis was performed at 25°C, and the same procedure was repeated at zeta potential. The prepared formulations zeta potential was characterized in order to determine their stability.

FESEM

FESEM can be used to determine the texture, surface topography, and fracture morphology. A FESEM (Carl Zeiss, supra55, Germany) at the central instrumental facility (Savitribai Phule Pune University) was used to assess the surface morphology of the curdlan nano formulation loaded with kaempferol. Samples were photographed using a different magnification power (10,000x).

Entrapment Efficiency (%EE)

The effectiveness of entrapment of the formulation of Kaempferol-loaded nanoparticles was assessed using the centrifugation method. For 30 minutes, 10 milligrams of the prepared nanoparticle formulation were centrifuged at 1400 rpm in an eppendorf (RM-12). A UV spectrophotometer set to 265 nm was used to analyze the liquid supernatant, which contained the drug that was not entrapped. It was then diluted with phosphate buffer pH 6.8. The absorbance entrapment efficiency (%EE) was calculated using the following formula.

Entrapment Efficiency percentage = $\frac{Total\ drug - free\ drug}{Total\ drug}$x100

Percentage of cumulative drug release

Using formulations containing 10 mg of kaempferol and kaempferol-loaded nanoparticles in phosphate buffer pH 6.8, a dissolution test was conducted using a USP type II dissolution test apparatus. A USP apparatus type-II was used to conduct the dissolution studies at 50 rpm and 37±0.5°C. There were 900 milliliters of dissolution media in the dissolution apparatus, and 10 mg of the medication was added to it. At 10, 20, 30, 40, 50, 60, 90, and 120 minutes, the 5 ml solution was removed, and the beaker was filled with an equivalent volume of phosphate buffer solution. The amount of dissolved drug was measured using UV-Vis spectroscopy at 265 nm.

Drug content

A volumetric flask containing 10 ml of weighed 10 mg Kaempferol-loaded curdlan nanoparticles was filled with methanol and subjected to a 15-minute sonication. A UV spectrophotometer (Jasco V-630) was then used to measure the percentage drug content at 265 nm after 1 ml of this mixture had been diluted to 10 ml with methanol. The calibration curve method was used to determine the drug content.

Stability studies

The curdlan nanoparticles loaded with kaempferol were stored both at 25 degree centigrade centigrade for room temperature and 2–8 degree centigrade for refrigerator at 90 days, or three months. Entrapment efficiency (EE%), drug content, and drug release percentage were computed.

Cytotoxicity assay

The cancer cell line MCF-7 and Hela was porcured from NCCS - National Centre for Cell Science, Pune, which were fostered by using 10 % fetal bovine serum (FBS) with EMEM (Eagle's Minimum Essential Medium). At 37 degree centigrade, air 95%, carbon dioxide 5%, and relative humidity 100 %, the cells were maintained. Maintenance cultures were passed once every seven days, and twice a week the culture medium was changed.

Technique for treating cells

EDTA Tetraacetic acid, trypsin, and ethylene diamine was employed for producing single-cell suspensions by separating the monolayer cells. In order to achieve A last thickness of $1x10^5$ cells per milliliter, viable cells which were diluted with a 10 % fetal bovine serum containing medium after being counted using a hemocytometer. Each well of well plates 96 received 100 microliters of cell suspension using 10,000 cells/well constituted the plating density. To enable cell attainable, the plates were subsequently incubated at 100 % relative humidity, 5 % carbon dioxide, 37 °C and 95 % air. The cells had been made the media to increasing concentrations of the assessment samples afterwards a day. Once disintegrating in clean dimethyl sulfoxide (DMSO), the final maximum test concentration can be doubled, A serum free medium was used to dilute a tiny amount of the sample solution.

To reach 5.0 sample concentrations, 4.0 additional serial dilutions were performed. To reach the necessary final sample concentrations of substances, 100 µl small amounts of each of these different sample dilutions were put into the corresponding wells, which already had 100 µl of medium in them. Following the addition of the sample, for further 48 hours, the plates were underwent incubation. at 95 % air, 5 % carbon dioxide, 100 % relative humidity, and 37 °C. Each concentration has been preserved in three duplicates, with the medium without of samples providing as the control.

MTT assay

Assay was done by using MTT reagent. It is an yellow colour tetrazolium salt that dissolves in water. The MTT becomes a formazan insoluble purple color when the tetrazolium ring breaks off in living cells by the mitochondrial enzyme succinate dehydrogenase. Thus, the quantity of formazan produced is directly proportional to the number of viable cells. Incubation was done by after 48 hours, 15 microlitre of MTT (5 mg/ml) in phosphate buffered saline (PBS) was was put into every well. Four hours the wells were then incubated at 37°C. 100 microliters of DMSO was used to dissolve the formed formazan crystals, after MTT containing medium was turned off. The absorbance at 570 nm was measured using a microplate reader. Determination of the percentage of cell viability compared to control using the following formula

$$\text{Percentage viability of cell} = \frac{Absorbance\ of\ test}{Absorbance\ of\ control} x100$$

% cell inhibition is calculated by

% Inhibition of cell = 100- Percentage viability of cell

GraphPad Prism software was used to calculate the IC50 and plot a graph of nonlinear regression between the log concentration and a percentage of cell inhibition.

RESULTS AND DISCUSSION

Experimental Design:

This study detailed the beneficial effects of curdlan nanoparticle formulations loaded with kaempferol. According to

the first trials, the most important factors influencing the drug content, encapsulation efficiency percentage, and invitro drug release were chitosan (mg) (A), sodium tripolyphosphate (B), and stirring speed (C). The Box-Behnken (BBD) [11] has good design qualities, is rotatable or nearly rotational, and has minute collinearity in the current design methods. Other approaches may be insensitive to missing data or have orthogonal blocks. Because of them, they find it difficult to predict at the boundaries of the design space. BBD is effective in identifying structuring second-order polynomial and quadratic response surfaces.

It is composed of a set of virtual center points located in the center of every boundary of a multi-dimensional cube. Thirteen runs were essential to the response surface approach, according to BBD. Table 1 shows the factor permutations that produced various responses. It goes without saying that each dependent variable is reliant on the selected independent variables. A large range of the 13 runs can be used to calculate this. The data was analyzed using Design-Expert Stat-Ease software (13.0 Version) to produce analysis of variance (ANOVA), regression equations, and regression coefficients.

Table 1:Suggested Experimental Runs Based on Box–Behnken Design

Run	Factor-1 Curdlan (mg)	Factor-2 Sodium Tripoly phosphate (mg)	Factor-3 Stirring Speed (RPM)	Drug content (%) (R1)	Entrapment efficiency (%) (R2)	Cumlative drug release (%) (R3)
1	30	3	1000	90.18	84.25	88.61
2	50	3	750	91.19	84.78	88.46
3	50	3.3	750	92.9	86.72	87.43
4	30	3.3	500	89.55	85.09	85.12
5	50	3.15	500	92.89	85.19	86.43
6	30	3.15	750	90.17	86.04	88.42
7	30	3	500	90.79	82.16	84.61
8	30	3.3	1000	89.71	85.17	86.27
9	50	3.15	1000	97.19	90.45	95.94
10	10	3.15	1000	92.47	86.17	90.01
11	10	3.3	750	88.89	87.3	84.84
12	10	3.15	500	95.35	88.16	91.54
13	10	3	750	90.16	85.67	87.56

%-Percentage, R1- Response 1, R2- Response 2, R3- Response 3

Table 2: Analysis of Variance Findings for Quadratic Model Response R1 (Drug Content)

Source	SS	Degree of freedom	MS	Fit value	Prob value	Findings
Model	69.49	9	7.72	11.69	0.0338	significant
A-Curdlan	6.66	1	6.66	10.09	0.0502	

B-Sodium Tripolyphosphate	0.2016	1	0.2016	0.3053	0.6191	
C-Stirring Speed	0.1176	1	0.1176	0.1781	0.7014	
AB	2.22	1	2.22	3.36	0.1641	
AC	12.89	1	12.89	19.52	0.0215	
BC	0.1482	1	0.1482	0.2245	0.6680	
A^2	14.47	1	14.47	21.92	0.0184	
B^2	8.26	1	8.26	12.51	0.0384	
C^2	7.31	1	7.31	11.08	0.0448	
Residual	1.98	3	0.6603			
Cor Total	71.47	12				

SS- Sum of Square, MS-Mean Square

Kaempferol-loaded curdlan nanoparticles have the drug content percentage between 88.89% to 97.19 %. The models F value of 11.69 showed that it was significant, and the Particle size factorial equation showed a good correlation coefficient 0.0500. In contrast to the clear erroneous there was a major insufficient match. as indicated by the lack of fit f-value of 11.69. A large lack of fit f-value was 3.38 % probably due to sound.

The ANOVA table summarizes the statistical analysis of a model involving three factors curdlan (A), Sodium Tripolyphosphate (B), and Stirring Speed (C) along with their interactions and quadratic effects. The model is statistically significant ($p = 0.0338$), indicating that at least one of the factors or interactions significantly affects the response variable. Among the individual terms, the linear effect of curdlan (A) is nearly significant ($p = 0.0502$), while sodium tripolyphosphate (B) and stirring speed (C) show no significant linear effects. However, the interaction between curdlan and stirring speed (AC) is significant ($p = 0.0215$), suggesting a combined influence on the response. Additionally, the quadratic terms C^2, B^2, and A^2 are all significant ($p < 0.05$), indicating that the response is notably influenced by nonlinear effects of each factor. The residual error is low (1.98), reinforcing the models goodness of fit. Overall, the analysis demonstrates that the model effectively captures key influences on the response, especially through interaction and quadratic effects.

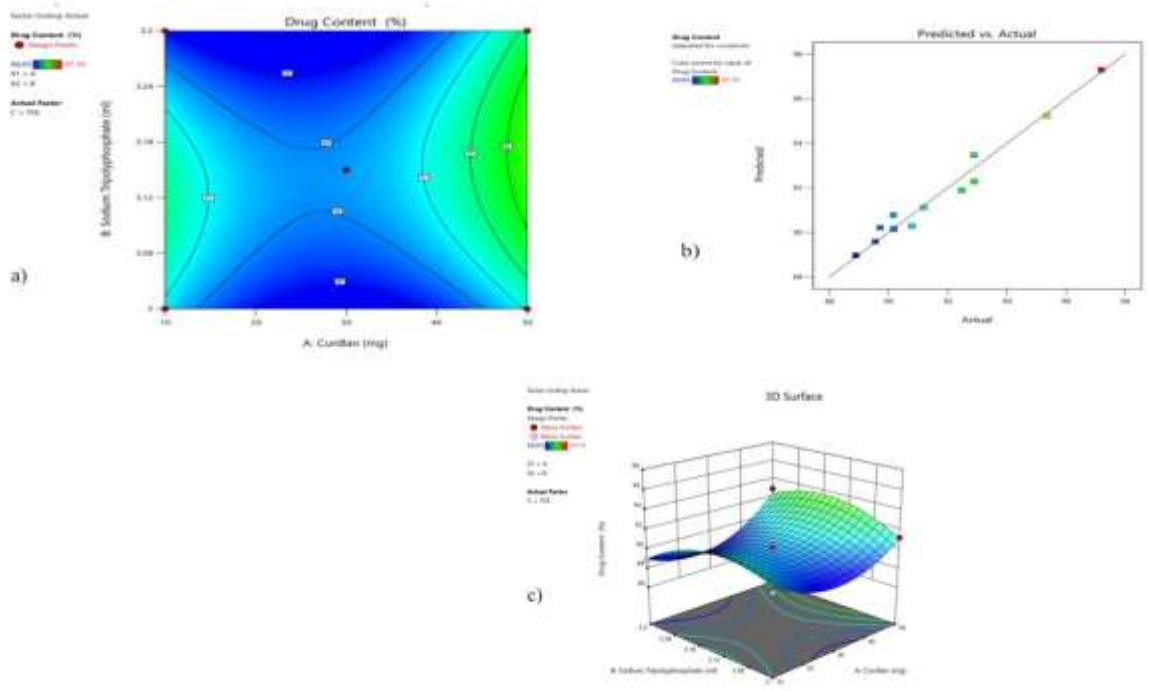

Figure : 1 (a) Contour Representation of Drug Content (%), (b) Predicted vs Observed Plot for Drug Content (%), and (c) 3D Surface Response Graph for Drug Content (%)

Graphical interpretation for Drug content

The three graphical plots collectively validate the effectiveness and reliability of the developed model for predicting drug content in the formulation [12]. The contour plot (2D) demonstrates that Curdlan (A) has a significant and nonlinear influence on drug content, while Sodium Tripolyphosphate (B) shows minimal effect; the highest drug content is achieved at higher Curdlan levels. The experimental and model-predicted values display a strong correlation in the predicted vs. actual plot, with the majority of the data points closely aligning along the diagonal, demonstrating the model's accuracy and low prediction error. Lastly, the 3D surface plot visually reinforces these findings, showing a curved surface that rises with increasing curdlan concentration, indicating strong quadratic and interaction effects, while the surface remains relatively flat across sodium Tripolyphosphate levels. Together, these plots confirm that curdlan plays a dominant role in enhancing drug content, and the model provides a good predictive fit.

The mechanism by which curdlan concentration influences drug content primarily involves its gel-forming capacity and viscosity enhancement. Curdlan, a β-1,3-glucan, forms a thermo-gelation matrix upon heating, which provides a structured environment for drug incorporation. At optimal concentrations, curdlan creates a uniform and stable polymer network that facilitates homogeneous drug dispersion and minimizes drug loss during processing. The increased viscosity associated with higher curdlan levels also slows down drug diffusion, thereby retaining more drug within the matrix and resulting in higher drug content. However, at very high concentrations, the overly dense gel may hinder proper mixing or entrapment, potentially leading to uneven drug distribution. Thus, an optimal curdlan concentration enhances drug content by balancing matrix strength and homogeneity, ensuring efficient drug loading and minimal loss.

Table 3: Analysis of Variance Findings for Quadratic Model Response R2 (Entrapment Efficiency)

Source	SS	Degree of freedom	MS	Fit value	Prob value	
Model	47.10	9	5.23	13.93	0.0264	significant
A-Curdlan	0.0032	1	0.0032	0.0085	0.9323	
B-Sodium Tripolyphosphate	6.88	1	6.88	18.32	0.0234	
C-Stirring Speed	3.70	1	3.70	9.85	0.0517	
AB	0.0240	1	0.0240	0.0639	0.8167	
AC	13.14	1	13.14	34.98	0.0097	
BC	1.01	1	1.01	2.69	0.1996	
A^2	6.62	1	6.62	17.61	0.0247	
B^2	6.03	1	6.03	16.04	0.0279	
C^2	0.1414	1	0.1414	0.3764	0.5829	
Residual	1.13	3	0.3757			
Cor Total	48.23	12				

SS- Sum of Square, MS-Mean Square

The overall model is statistically significant, according to the ANOVA table ($p = 0.0264$), suggesting that the combination of factors meaningfully affects the response variable [13]. Among the individual factors, sodium tripolyphosphate (B) and stirring speed (C) show relatively strong effects, with B being statistically significant ($p = 0.0234$) and C nearly significant ($p = 0.0517$). The interaction between curdlan and stirring speed (AC) is highly significant ($p = 0.0097$), highlighting a strong synergistic effect between these two variables. Quadratic effects for both B^2 and A^2 are also significant ($p = 0.0279$ and 0.0247, respectively), indicating the presence of curvature in the response. In contrast, curdlan (A) alone and other interaction terms (AB, BC) and C^2 are not significant, suggesting they have minimal individual influence. The low residual error (1.13) supports the models good fit, and the findings collectively show that B (sodium tripolyphosphate), its interaction with C, and the quadratic terms are key contributors to the variation in the response. The importance of the model was based on its the value of f -13.93. and a good correlation coefficient of 0.0500 was found in the entrapment efficiency factorial equation. The probability that an f-value this high might be brought on by noise alone 2.64 %.

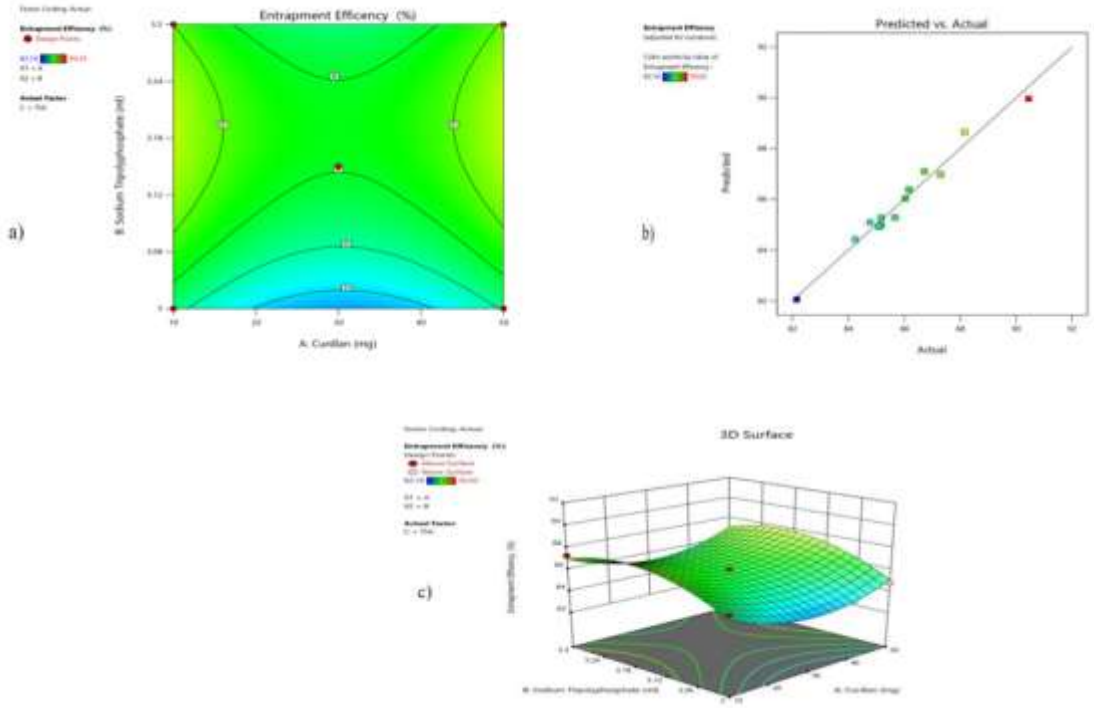

Figure : 2 (a) Contour Representation of Entrapment Efficiency (%), (b) Predicted vs Observed Plot for Entrapment Efficiency (%), and (c) 3D Surface Response Graph for Entrapment Efficiency (%)

Graphical interpretation for Entrapment Efficiency

The three graphs collectively illustrate the influence of formulation variables curdlan and sodium Tripolyphosphate (STPP) on Entrapment Efficiency (%) [14]. The 2D contour plot shows how variations in curdlan and STPP concentrations affect entrapment efficiency, with higher values seen in the region where both factors are moderately elevated, suggesting a synergistic interaction. The predicted vs. actual plot indicates a strong correlation between experimental and model-predicted values, as most data points lie close to the diagonal line, affirming the models accuracy and predictive reliability. The 3D surface plot further visualizes this relationship, revealing a rising plane of entrapment efficiency as both curdlan and STPP increase, especially highlighting the critical role of STPP in cross-linking and stabilizing the polymer matrix. Together, these plots confirm that optimized levels of curdlan and STPP significantly enhance drug entrapment, with the model effectively capturing these effects.

Curdlan concentration and Sodium Tripolyphosphate (STPP) play complementary roles in enhancing entrapment efficiency. Curdlan, a gel-forming polysaccharide [15-16], contributes to the formation of a robust matrix that physically encapsulates the drug, with increasing concentrations improving viscosity and structural integrity up to an optimal point. Meanwhile, STPP acts as a cross-linking agent, interacting electrostatically with curdlan to strengthen the polymer network and reduce drug leakage. The statistical and graphical analyses indicate that while curdlan alone has a limited direct effect, its interaction with STPP significantly improves entrapment efficiency. This synergistic effect ensures that as both curdlan and STPP concentrations increase within an optimal range the matrix becomes more cohesive and efficient at trapping the drug, resulting in higher entrapment efficiency.

Table 4: Analysis of Variance Findings for Quadratic Model Response R3 (cumulative drug release)

Source	SS	Degree of freedom	MS	Fit value	Prob value	Findings
Model	113.65	9	12.63	16.10	0.0215	significant
A-Curdlan	2.32	1	2.32	2.96	0.1838	
B-Sodium Tripolyphosphate	3.89	1	3.89	4.96	0.1122	
C-Stirring Speed	21.55	1	21.55	27.47	0.0135	
AB	0.7140	1	0.7140	0.9103	0.4104	
AC	30.47	1	30.47	38.85	0.0083	

BC	2.03	1	2.03	2.59	0.2060	
A^2	6.92	1	6.92	8.82	0.0591	
B^2	21.79	1	21.79	27.78	0.0133	
C^2	1.54	1	1.54	1.96	0.2561	
Residual	2.35	3	0.7843			
Cor Total	116.01	12				

SS- Sum of Square, MS-Mean Square

According to the ANOVA table, the overall model successfully explains response variation and is statistically significant (p = 0.0215). Among the individual factors, stirring speed (C) and the interaction between curdlan and stirring speed (AC) are statistically significant (p = 0.0135 and 0.0083, respectively), showing they have a strong influence on the response. Additionally, the quadratic effect of sodium tripolyphosphate (B^2) is significant (p = 0.0133), suggesting a non-linear relationship. Other factors such as curdlan (A), sodium tripolyphosphate (B), their interaction (AB), and other squared terms are not statistically significant, indicating they have limited or no impact within the tested range. The model was significant, based on its the value of f -16.10. The probability that an f-value this high might be brought on by noise alone 2.15 %.

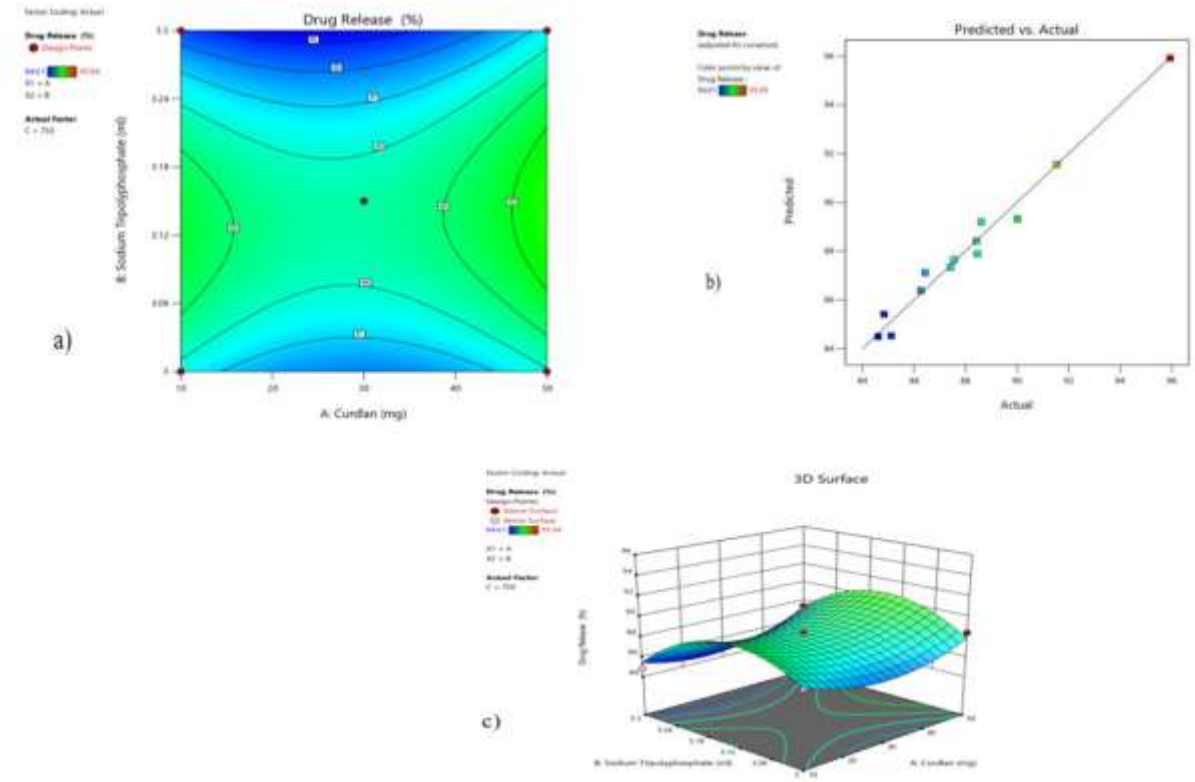

Figure : 3 (a) Plot Contour for Drug Release (%), (b) Predicted vs Actual plot for Drug Release (%), (c) 3D Response Surface plot for Drug Release (%)

Graphical interpretation for percentage Drug Release

The contour plot, 3D surface plot, and predicted vs. actual plot collectively demonstrate how curdlan (A) and sodium tripolyphosphate (B) influence drug release at a fixed stirring speed (C = 750 rpm). The 3D and contour plots reveal a curved surface, indicating a non-linear relationship and significant interaction (especially AC) influencing the drug release, with maximum drug release observed at higher levels of curdlan. The curvature also supports the significance of the quadratic term B^2, as shown in the ANOVA. The predicted vs. actual plot displays a strong correlation along the diagonal, indicating that the model accurately fits the experimental data and reliably predicts drug release percentages**.**

Stirring speed and curdlan concentration significantly influence drug release by affecting the matrix structure and drug entrapment efficiency. Higher stirring speeds during formulation enhance shear force, resulting in smaller particle sizes and more uniform dispersion of curdlan, which leads to a tighter and more consistent gel matrix that can control and sustain drug release. On the other hand, increasing curdlan concentration thickens the gel matrix, reduces porosity, and enhances the barrier to drug diffusion, thereby slowing down the release rate. However, excessive curdlan can overly restrict drug mobility, while insufficient stirring may result in heterogeneous matrices and irregular drug release. The combined effect of optimized stirring speed and curdlan concentration ensures a well-structured matrix that enables controlled, sustained drug release.

Table 5: Regression Model Equations for Experimental Responses

Response Regression equation
R1= +90.17+0.9125A-0.1588B+0.1212C+0.7450AB+1.79AC+0.1925BC+2.52A²-1.90B²+1.79C²
R2=+88.42+0.5387A--0.6975B+1.64C+0.4225AB+2.76AC-0.7125BC+1.74A²-3.09B²+0.8200C²
R3=+88.42+0.5387A--0.6975B+1.64C+0.4225AB+2.76AC-0.7125BC+1.74A²-3.09B²+0.8200C²

R1- Drug content, R2- Entrapment efficiency , R3- cumlative drug release

R-squared is the coefficient of determination. Since it is a ration of the fraction of the total squared error,the value of R^2 ranges from zero to one. It is better if the value is closer to one. Nevertheless, a large value of R^2 does not certainly denote a good regression model. Adding a variable to the model will always increase, regardless of the statistical significance of the additional variable, R^2 will be increased if available is added into the model. The Adjusted R-squared statistic is crucial in which its value falls if pointless variables are incorporated. The regression equation for all responses were shown in table 5.

The existence of extraneous terms can be implied when the two statistics are used together in the computed model which a large difference between the values of R^2 and Adj^2 is greater than 0.2. Residual is the difference in the amount of estimated output and the real output. PRESS is a measurement of the extent of the model suits individual aspect in the design. Predicted R^2 can be calculated by PRESS. Adeq precision is applied to measure the signal to noise ratio. Preferably, the ratio should be more than four. Adequate precision showed (R1, R2, R3) was 11.16950, 14.7092 and 14.7071 shows sufficient signal individually. This model can be used to navigate the design space. These statistics are employed with an intention of avoiding over suiting of model. ANOVA derived statistical parameters and reduced response surface models were shown in table 6.

Table 6: Statistical Parameters Obtained from ANOVA and Simplified Response Surface Models

Interactions	R^2	Adjusted R^2	Predicted R^2	Adeq Precision
R1	0.9723	0.8891	0.9012	11.6950
R2	0.9766	0.9065	0.9154	14.7092
R3	0.9797	0.9189	0.9276	14.7071

R^2,Adjusted R^2,Predicted R^2 and Adequate Precision- Anova values

The KF9 batch code of Kamfperol loaded curdlan nanoparticles formulated following the construction of the polynomial equations connecting the dependent and independent variables, in accordance with the optimized levels. By placing restrictions on the dependent and independent variables, the optimization conditions were obtained. The observed values closely matched the optimized process expected values. The KF9 formulation % drug content, efficiency entrapment % and drug release cumulative % has been found to be 97.19, 90.45 % and 95.94 ±0.28. The KF9 formulation demonstrates favorable characteristics in terms of size of the particle, Poly dispersity Index, and zeta potential. The size of the particle of 157.4 nm suggests that the formulation is within an optimal range for drug delivery, ensuring efficient absorption and stability. The poly dispersity index value of 0.248 indicated a narrow distribution of particle sizes, which is ideal for formulation uniformity. Additionally, the zeta potential of -25.9 mV reflects good colloidal stability, as the negative charge helps prevent aggregation of nanoparticles. These properties suggest that KF9 was a promising formulation with suitable characteristics for effective drug delivery applications.

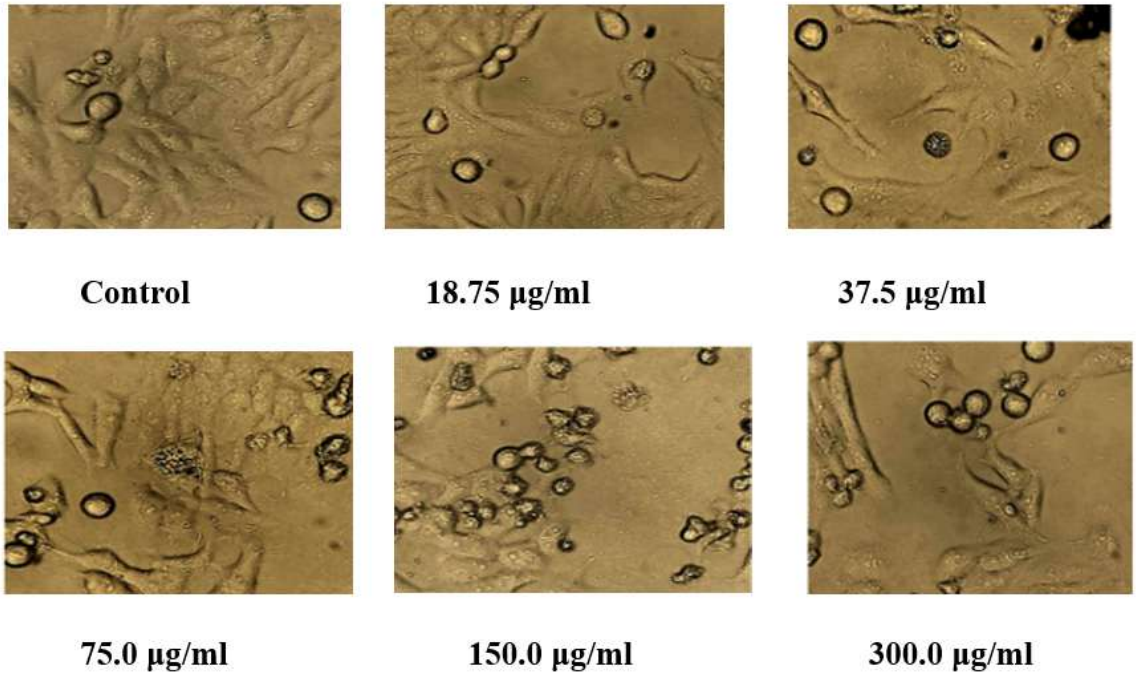

Figure 4: Cell Viability and Cytotoxicity Images of MCF-7 Cell Line

Table 7: Inhibitory Activity Results Against MCF-7 Breast Cancer Cell Line

Conc (µg/ml)	Average absorbance	% inhibition	IC50 value
18.75	0.370±0.115	19.16	73.02 µg/ml
37.5	0.295±0.097	35.46	
75.0	0.225±0.175	50.80	
150.0	0.178±0.329	65.90	
300.0	0.095±0.230	79.57	
Control	0.454±0.169		

n=3, Mean±Stand Deviation, %inhibition- Percentage inhibition IC50- Inhibitory Concentration

The provided images depict the effect of different concentrations of a treatment on MCF-7 breast cancer cells under a microscope. The control image shows healthy, well spread cells with normal morphology. As the concentration increases from 18.75 to 37.5 µg/ml and higher, there is a clear dose-dependent cytotoxic effect, evident by the increasing number of rounded, detached, and possibly apoptotic or necrotic cells. The treated cells show signs of cell death such as shrinkage, loss of adherence, and cellular debris, indicating that the treatment effectively inhibits the proliferation and concentration-dependent survival of MCF-7 the breast carcinoma cells [17-18]. The data in Table 7 demonstrates the dose-dependent inhibitory effect of the tested sample on breast cancer cells MCF-7. As the concentration increases from 18.75 to 300 µg/ml, the average absorbance decreases while the percentage inhibition correspondingly increases, indicating greater cytotoxicity at higher doses. The control group, with an absorbance of 0.454, shows no inhibition. The calculated IC50 value of 73.02 µg/ml reflects the concentration at which 50% inhibition of cell viability occurs, highlighting the sample's moderate potency against MCF-7 cells. This trend confirms that increasing the concentration effectively reduces cell viability, supporting the potential anticancer activity of the tested compound.

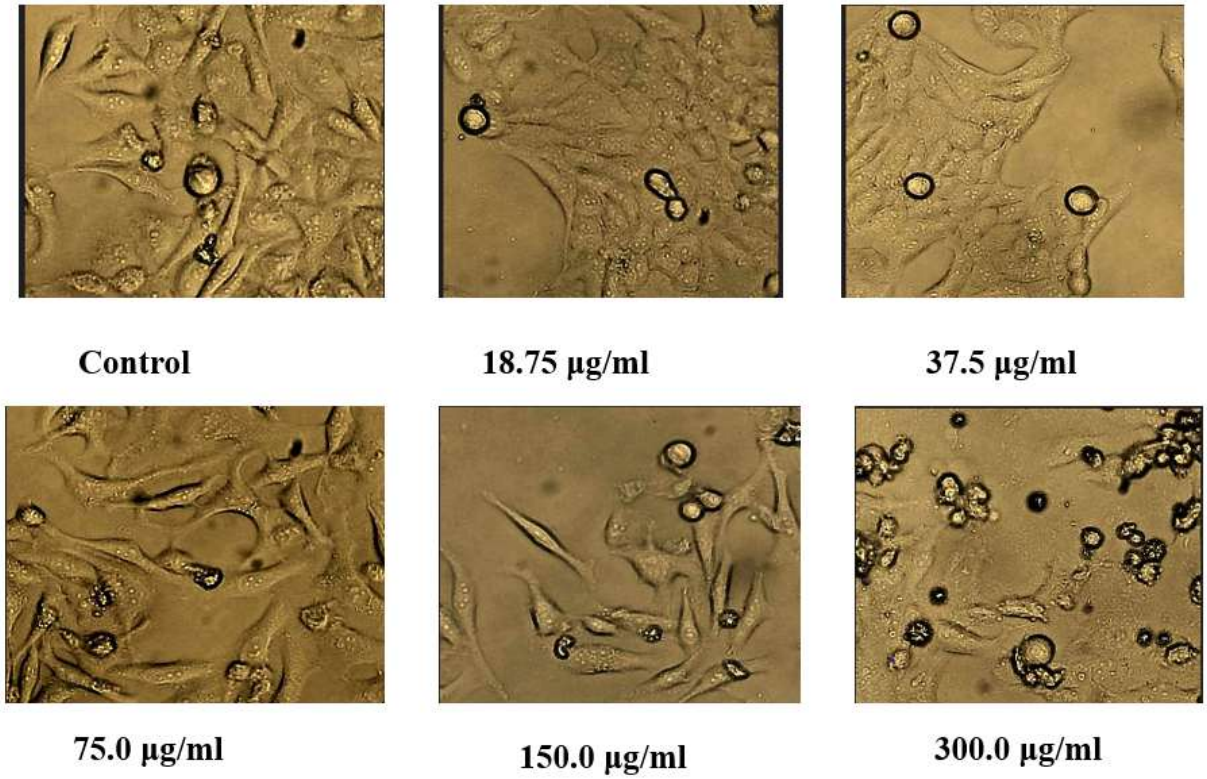

Figure 5: Cell Viability and Cytotoxicity images for Hela cell line

Table 8 : Inhibitory Activity Results Against Hela cervical Cancer Cell Line

Conc (µg/ml)	Average absorbance	%inhibition	IC50 value
18.75	0.355±0.259	16.66	84.83 µg/ml
37.5	0.289±0.125	33.39	
75.0	0.230±0.146	49.20	
150.0	0.177±0.219	59.90	
300.0	0.102±0.309	77.10	
Control	0.426±0.220		

n=3, Mean±Stand Deviation, %inhibition- Percentage inhibition IC50- Inhibitory Concentration

The microscopic images illustrate the morphological changes in HeLa cells (cervical cancer cell line) treated with increasing concentrations of a test compound. The control group exhibits dense, healthy, and elongated cells with intact morphology. At 18.75 and 37.5 µg/ml, a slight reduction in cell density and early signs of cell shrinkage can be observed. As the concentration increases to 75.0 µg/ml and 150.0 µg/ml, noticeable cytotoxic effects become apparent, including loss of adhesion, membrane blebbing, and cellular deformation. At the highest concentration of 300.0 µg/ml, cells appear severely damaged or lysed, with widespread cell death and fragmented debris dominating the field [19-20]**.** These images confirm a concentration-dependent cytotoxic effect of the compound on HeLa cells, suggesting its potential efficacy in inhibiting cervical cancer cell proliferation.

The data for the HeLa cell line (cervical cancer study) shows a clear concentration-dependent inhibition of cell viability upon treatment with the test compound. The control group, with an average absorbance of 0.426, indicates

healthy and viable cells without any treatment. As the concentration increases from 18.75 to 300.0 µg/ml, the average absorbance consistently decreases, reflecting a progressive decline in viable cells. Correspondingly, the percentage inhibition increases from 16.66 % at the lowest dose to 77.10 % at the highest, indicating enhanced cytotoxicity with higher concentrations. The IC50 value calculated as 84.83 µg/ml represents the concentration at which 50 % inhibition is achieved, signifying moderate anticancer potential of the compound against HeLa cells. These results confirm the effectiveness of the sample in suppressing cervical cancer cell growth in a dose-dependent manner.

CONCLUSION

In conclusion, optimization and validation of kaempferol-loaded curdlan nanoparticles using the Box–Behnken design proved to be an effective approach for optimizing formulation parameters to achieve maximum drug entrapment efficiency, controlled release, and desirable nanoparticle attributes. Statistical modeling confirmed the significant influence of formulation variables such as curdlan concentration, sodium tripolyphosphate (TPP), and stirring rate on key response outcomes like drug content and entrapment efficiency. The resulting nanoparticles exhibited favorable physicochemical characteristics, including optimal particle size, surface charge (zeta potential), and morphology, which are essential for enhanced stability and cellular uptake. Significant cytotoxic effects were shown in in vitro anticancer evaluations with the MCF-7 protein and the HeLa cells cell lines, using IC_{50} values of 73.02 and 84.83 µg/ml, respectively, indicating a dose-dependent inhibition of cancer cell proliferation. These findings highlight the potential of curdlan, a biocompatible and biodegradable polysaccharide, as a promising carrier for the efficient delivery of poorly soluble phytochemicals like kaempferol. Overall, the study underscores the potential of this nanoformulation as a safe, effective, and targeted drug delivery system worthy of further exploration in preclinical and clinical cancer research.

Acknowledgement

The provided research facilities and the encouragement given in completing the novel Vels Institute of Science and Technology and Advanced Studies, Pallavaram, Chennai, Tamilnadu, deserves a gratitude from the authors

Conflict of Interest statement

No conflicts of interest were disclosed by the authors

Author contributions

Each author made a substantial contribution to this work, took part in its review and editing, and gave their approval for the publication of the final draft.

REFERENCES

1. Zeenat Ayoub, Archana Mehta, Siddhartha Kumar Mishra. Ethnopharmacological review of natural products in cancer prevention and therapy. Asian J Pharm Clin Res. 2018;11(7):342–349.
2. Settu K**,** Vaiyapuri M. Formulation and evaluation of isorhamnetin-loaded PLGA nanoparticles. Asian J Pharm Clin Res. 2017;10(1):177–181
3. Eduardo Fernandes de Morais, Marcelo de Andrade Vieira, Wendel Silva Nascimento, Elenilson Gurgel Pereira, Renan Demarque de Campos, Hélio Mágno da Silva Nogueira, Ivanildes da Silva Araújo, André Luiz Macedo, Márcio Bezerra da Silva. The Anticancer Potential of Kaempferol: A systematic review based on in vitro studies. Cancers, 2024; 16(3): 585. https://doi.org/10.3390/cancers16030585.
4. Sukhmandeep Kaur, Priscilla Mendonca, Khalid Fakhrood Soliman. The Anticancer effects and therapeutic potential of Kaempferol in triple-negative breast cancer. Nutrients, 2024; 16(15): 2392. https://doi.org/10.3390/nu16152392
5. Jing Zhang, Yu Zhang, Xiaojie Zhang, Wei Zhou, Yingzi Luo, Ziqiang Xie, Yiran Yang, Yangyi Bao, Bin Zhang. To explore the effect of kaempferol on non-small cell lung cancer based on network pharmacology and molecular docking. Front Pharmacol, 2023;14: 1148171. https://doi.org/10.3389/fphar.2023.1148171
6. Hamed Reza Nejabati, Laya Roshangar. Kaempferol: A potential agent in the prevention of colorectal cancer. Physiolo Reports. 2022; 10(20): e15488. https://doi.org/10.14814/phy2.15488
7. Himanshu Bera, Yasir Fayyaz Abbasi, Anil Thakur. Curdlan/Clay nanocomposite-reinforced alginate beads as drug carriers. J Poly Environ. 2024; 32: 854–869. https://doi.org/10.1007/s10924-023-03036-0.
8. Meng Zhang, Xiaojing Sun, Feng Chen, Qiang Zhang, Xiaowen Zhang. . Curdlan-based drug delivery systems: A review. Inter J Biolog Macromole. 2020;155: 626–636. https://doi.org/10.1016/j.ijbiomac.2020.03.201
9. Zhi Liu, Shuting Li, Xiaocheng Song, Yingpeng Zeng, Xiang Li. Recent progress in the development of β-glucan-based drug delivery systems. Carbohy Poly. 2023; 311: 120767. https://doi.org/10.1016/j.carbpol.2023.120767

10. Hyun Seok Shin, Dong Soo Lee, Seung Jin Lee. Biomedical applications of curdlan and curdlan derivatives. Carbohy Poly. 2013; 93(1): 355–361. https://doi.org/10.1016/j.carbpol.2012.06.065
11. Surendra Singh Raghav, Vijay Thakur, Ankush Kumar, Pawan Kumar, Anurag Verma. Development and optimization of kaempferol-loaded ethosomes using Box-Behnken statistical design: In vitro and ex-vivo assessments. J Drug Del Sci Tech. 2024; 84: 104577. https://doi.org/10.1016/j.jddst.2024.104577
12. Mohammad S. Algahtani, Arshad Ali Khan, Saad M. Alkahtani, Mohammad A. Almohizea, Mohd Abul Kalam. Development of a Curcumin-loaded Lecithin/Chitosan nanoparticle utilizing a Box-Behnken design of experiment: formulation design and influence of process parameters. Polymers. 2022; 14(18): 3758. https://doi.org/10.3390/polym14183758
13. Mohd Abul Kalam, Arif Nawaz, Mohd Wajid Ali Khan, Zeenat Iqbal, Firoz Anwar, Yasir Mohd. (2016). Optimizing indomethacin-loaded chitosan nanoparticle size, encapsulation, and release using Box-Behnken experimental design. Inter J Bio Macromole. 2016; 87: 329–340. https://doi.org/10.1016/j.ijbiomac.2016.02.033
14. Ammar S. Zidan, Fahmy A. Fahmy, Wafaa S. Aljaeid, Amani A. Shehata. Optimization of methotrexate loaded niosomes by Box-Behnken design: An understanding of solvent effect and formulation variability. Drug Develop Ind Pharm. 2017; 43(9):1450–1459. https://doi.org/10.1080/03639045.2017.1318907.
15. Kumar SK, Manju V. Nanoparticle formulation of bioflavonoids for enhanced anticancer activity. Int J Appl Pharm. 2022;14(2):15–21.DOI: 10.22159/ijap.2020v12i5.38425
16. Ilk S**,** Sağlam N, Özgen M, Korkusuz F, Sa N. Chitosan nanoparticles enhance the anti-quorum sensing activity of kaempferol. Int J Appl Pharm. 2021;13(4):45–52. https://doi.org/10.1016/j.ijbiomac.2016.10.068
17. Raghavan BS, Kondath S, Anantanarayanan R, Rajaram R. Kaempferol-mediated synthesis of gold nanoparticles and their cytotoxic effects on MCF-7 cancer cell line. Asian J Pharm Clin Res. 2023;16(4):245–251.https://doi.org/10.1016/j.procbio.2015.08.003
18. Wei-Yi Qiu, Qiong Wu, Zhi-Chuan Zhang, Yi-Yu Lu, Zhi-Yong Qian. pH dependent green synthesis of gold nanoparticles by completely C6-carboxylated curdlan under high temperature and various pH conditions. Inter J Bio Macromole. 2018; 106: 498–506.https://doi.org/10.1016/j.ijbiomac.2017.08.029.
19. Luo H**,** Jiang B, Li B, Li Z, Jiang BH, Chen YC. Kaempferol nanoparticles achieve strong and selective inhibition of ovarian cancer cell viability. Int J Appl Pharm**.** 2019;11(3):110–118. DOI: 10.2147/IJN.S33670
20. Balasundaram S. Raghavan, Sivarama Krishna Lakkakula, Soundararajan Bangaru. Kaempferol mediated synthesis of gold nanoparticles and their cytotoxic effects on MCF7 cancer cell line. Process Biochem. 2015; 50(12): 1966–1976. https://doi.org/10.1016/j.procbio.2015.08.003**.**